PROCEEDINGS OF SCIENCE

Calibration of the gravitational wave telescope KAGRA

Dan Chen[a,*] **on behalf of the KAGRA collaboration**

[a] *Kamioka Branch, National Astronomical Observatory of Japan, 238 Higashi-Mozumi, Kamioka-cho, Hida City, Gifu 506-1205, Japan*

E-mail: dan.chen@nao.ac.jp

KAGRA is a laser interferometric gravitational wave (GW) telescope in Japan. It joined O4, the fourth international GW observation run, with other telescopes, namely, Laser Interferometer Gravitational Wave Observatory (LIGO) and Virgo. In the previous GW observation runs: O1, O2, and O3, 90 events were reported, and many more events are expected to be observed in O4. With the beginning of GW astronomy, the calibration of observed GW signals is becoming more important than ever before. The main calibration system used in KAGRA, LIGO, and Virgo is a photon calibration system (Pcal), which injects reference signals into a telescope by the radiation pressure of a laser. On the basis of the preparation and operation of KAGRA Pcals in O3, we prepared an upgrading plan for O4. This plan includes three main improvements: improving the Pcal laser beam alignment system, reducing noise, and dereasing uncertainty. Improvement works were conducted between the end of O3 and the start of O4 in accordance with this plan. The following results were obtained: first, precise remote alignment was enabled in the critical Pcal laser path region. Second, a Pcal noise source was identified and noise was significantly improved, resulting in a remarkable 50 dB reduction and sufficient reduction of the Pcal noise below the design sensitivity of KAGRA. Third, studies on the temperature dependence and laser incidence state dependence of the integrating sphere-type power meter were conducted to reduce the uncertainty of the Pcal, which is directly related to the uncertainty of the telescope signal. The details of the KAGRA Pcal and the improvements made between O3 and O4 are reported in this study.

38th International Cosmic Ray Conference (ICRC2023)
26 July - 3 August, 2023
Nagoya, Japan

*Speaker

PoS(ICRC2023)1549

1. Calibration of the gravitational wave telescope KAGRA

On Sep. 14 2015, the Laser Interferometer Gravitational Wave (GW) Observatory (LIGO) accomplished the first direct detection of GWs; this event marked the beginning of GW astronomy [1]. Since then, three observation runs have been conducted. We are currently in the midst of O4, the fourth international joint observation run, which started in May 2023. A total of 90 GW events were reported by the third observation run (O3). These events included the first multimessenger binary neutron star merger event kicked by a GW detection, GW170817 [2]. As the number of observations continued to increase, the observational accuracy became as important as the detectability of GWs. In the field of multimessenger astronomy, which incorporates follow-up observations using optical telescopes, the precise localization estimation of GW sources has become crucial.

Increasing the number of operating telescopes not only increases detection frequency detection but also improves source localization estimation. KAGRA is a laser interferometer-type GW telescope built in Japan. It started operating in 2019 and is currently participating in O4. Although KAGRA still has lower sensitivity than LIGO or Virgo, it continues to be upgraded to contribute to the GW observation network to increase the number of telescopes making simultaneous observations and expand the coverage of sensitive observation areas.

The KAGRA interferometer has numerous real-time control loops to maintain it in a highly sensitive state. In particular, the differential arm (DARM) control loop (Figure 1), which may contain the GW signal is the most important calibration target.

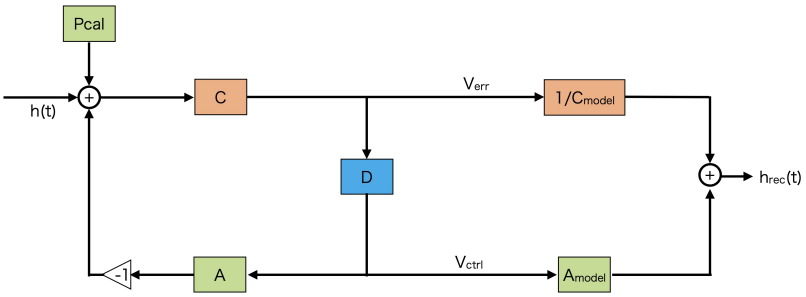

Figure 1: Differential arm (DARM) control loop and the h(t) reconstruction. The DARM control loop, consisting of sensor C, control filters D and actuator A, is the most important control loop for gravitational wave (GW) detection. The numerical model of C and A, error signal $V_{\rm err}$ and control signal $V_{\rm ctrl}$ are used to reconstruct the strain information, which may include GW signals.

The DARM control loop is a negative feedback system. It is composed of sensor C or the interferometer; control filters D; and actuators A, which are coil magnet actuators on an end mirror or the end test mass (ETM) of the interferometer. We use the output signal from C (error signal $V_{\rm err}$), signal into A (control signal $V_{\rm ctrl}$), and the model of C and A ($C_{\rm model}$ and $A_{\rm model}$) to reconstruct the injected signal that may contain the GW signal $h(t)$, as shown in Figure 1. $h_{\rm rec}(t)$ is the main output data of the telescope, which is called reconstructed strain data. Photon calibration systems (Pcals) are used as the primary calibrators in KAGRA and other telescopes [3]. A Pcal is a calibrated actuator that can inject signals into the interferometers to measure the transfer function of C and A for modeling. We have upgraded the Pcal after O3GK, a joint observation run by KAGRA and GEO 600, in 2020 [4].

2. Photon calibration system

2.1 Photon calibration system: Pcal

A Pcal is a system that injects laser beams into an ETM to make a displacement with the laser radiation pressure. In KAGRA, independent Pcals are installed for each of the two ETMs, ETMX and ETMY: Pcal-X and -Y. These systems have the same concept design. Pcal-X is used as the main calibration system, and Pcal-Y is the backup system. Although the following mainly describes Pcal-X, the improvements described below were applied to Pcal-X and -Y. Figure 2 shows the concept of a Pcal, which consists of a transmitter (Tx) module, generating laser beams and controlling power, and a receiver (Rx) module, receiving the laser beams reflected by the ETM. The two Pcal laser beams have a wavelength of 1047 nm and are generated by a continuous wave ytterbium fiber laser source (KEOPSYS by Lumibird). They are injected into a noncentered suitable point on the ETM to avoid exciting the internal resonant mode. Each beam passes through an acousto-optic modulator (AOM) and is extracted using by a beam sampler into photodetectors (PDs) called optical follower servo (OFS) PD and Tx PD at a 0.4% ± 0.07% power of the injection power [5] (Figure 2). The output of the OFS PD is input of a control filter and an AOM as an actuator for laser power to configure a laser power stabilization system, which is necessary to provide reference signals without substantial noise injection. The control system has an input port, where the laser power is controlled by following the voltage signal input. For this reason, this control system is called the OFS system. The two beams are injected into a vacuum chamber through an optical window and aligned toward the ETM by some mirrors in A chamber, reflected into the Rx module, and then received by the Rx PD. Integrating sphere type laser power meters are used for the Tx and Rx PDs to accurately and precisely measure the Pcal laser power. Given the conditions of the installation site, the Pcal system was installed in the A chamber area 34.9 m away from the ETM, making beam alignment difficult.

The displacement generated by the Pcal is presented by the following equation [3]:

$$x(f) = -\frac{2P(f)\cos\theta}{cM(2\pi f)^2}\left[1 + (\vec{a}\cdot\vec{b})\frac{M}{I}\right], \tag{1}$$

where $x(f)$ is the displacement in the frequency domain; P is the total Pcal laser power on the ETM; θ is the incident angle; c is the speed of light; M is the mass of the ETM; $\vec{a}$ and $\vec{b}$ are the position vector on the ETM of the sum of the Pcal beams and the main interferometer laser beam, respectively; and I is the moment of inertia of the mirror.

Interferometer calibration is performed in the frequency domain. Therefore, sinusoidal waves are injected into the interferometer using the Pcal. For this purpose, the Pcal laser power is held at a certain DC value and added with the sinusoidal waves. The sinusoidal waves are always input as reference signals when the telescope is in observation mode.

The signal from the Pcal is used as a reference for interferometer calibration such that the uncertainty of the Pcal itself directly affects the uncertainty of the telescope. From Equation 1, we can estimate the extent to which the uncertainty in the measurement of each parameter value affects the uncertainty of the Pcal. The measurement uncertainty of laser power measured at the Rx PD, and the Tx PD is the most particularly dominant. This situation accounts for the need for accurate and precise absolute calibration of integrating spheres.

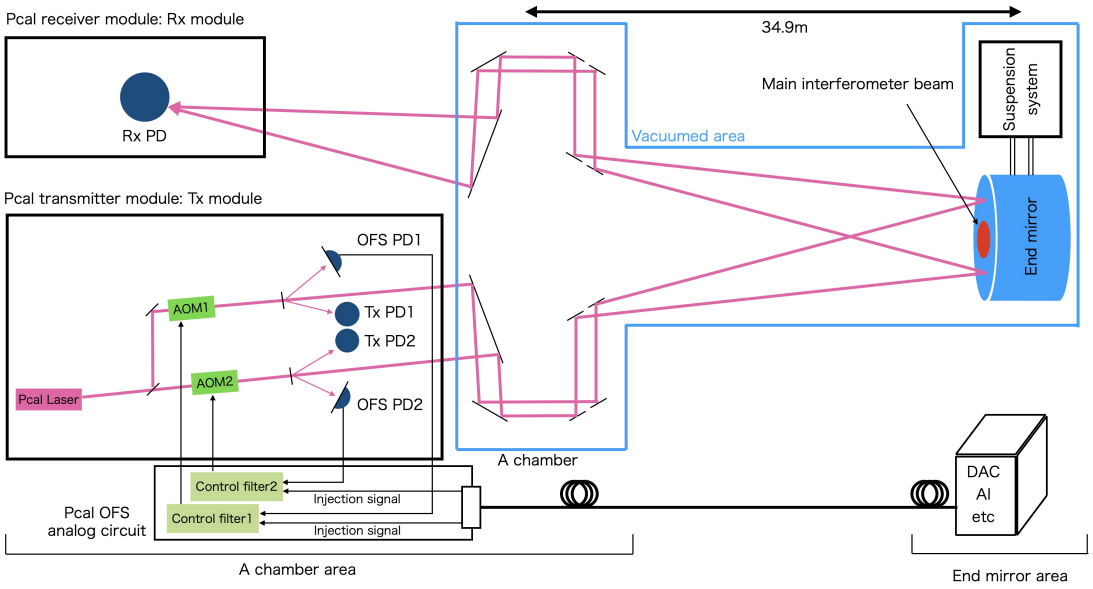

Figure 2: KAGRA Pcal, which is the primary calibration system injecting the reference signal by laser radiation pressure. OFS systems are implemented in the Tx module to inject power-controlled lasers. The Pcal laser power is measured by the Tx PDs and the Rx PD to estimate the end mirror displacement applied by the Pcal, which is the reference signal. The OFS systems are controlled by the KAGRA real-time system through a digital-analog converter and anti-imaging filters. The A chamber area and the end mirror area are separated by a distance of 34.9 m.

2.2 Integrating sphere calibration

For the calibration of integrating spheres, the LIGO group calibrates the standard integrating sphere gold standard of KAGRA (GSK), which is based on the integrating sphere gold standard of LIGO (GSL) that is absolutely calibrated by the National Institute of Standards and Technology (NIST) [3] [6]. The GSK is maintained at the University of Toyama and acts as the standard laser power meter in KAGRA. For calibrating integrating spheres at the KAGRA site, such as the Rx PD, another integrating sphere, called working standard of KAGRA (WSK) is used to carry the calibration factor from the GSK at the University of Toyama to the KAGRA site. This work is conducted about once a month to monitor long-term changes in the calibration factor of each integrating sphere in KAGRA. When calibrating the WSK with the GSK, we essentially adopt the method described in a previus work [3]: We inject a laser separated by a beam splitter into the GSK and WSK and measure the output ratio of the two integrating spheres [7]. Figure 3 illustrates the calibration procedure for integrating spheres. A global network for the calibration of GW telescopes that includes not only NIST but also Die Physikalisch-Technische Bundesanstalt (PTB) as a standard orbit is planned to improve reliability of the integrating sphere calibration [6].

2.3 Issues and points of enhancement found by O3GK

We performed Pcal installation and basic operation by O3GK [4]. The following issues and points for improvement were found during the installation and operation.

A. Difficulty of beam alignment and beam position adjustment on the ETM

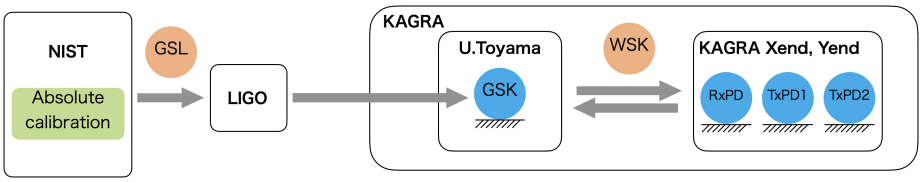

Figure 3: Procedure for integrating sphere calibration. NIST provides an absolute calibration of one integrating sphere, and we transport that calibration to the KAGRA site via several comparison calibration measurements. Arrows indicate transport of integrating spheres.

B. Noise in the main interferometer caused by the Pcal

C. Improvements in calibration uncertainty

A: The first issue is related to the work efficiency of Pcal beam alignment. As indicated above, we need to perform a round-trip laser beam alignment of ~70 m. This 70-m component is a vacuum pipe. Given that entering and checking the beam position is difficult, a delicate alignment from the A chamber area is required. During O3GK, we lacked an effective alignment system for this 70-m component. In addition, after vacuuming, the Pcal beam positions still need fine tuning. However, a mechanism that could efficiently perform this action is unavailable.

B: The second point focuses on the noise in the interferometer caused by the Pcal. After O3GK, the noise of Pcal-X was checked and found to be greater than expected. It exceeded the designed sensitivity of KAGRA and may limit sensitivity during O4. During the observation run, the Pcal continues to input reference signals to the interferometer; however, it is assumed to be nonfunctional at other frequencies.

C: The last point is the improvement in the uncertainty of the Pcal. Such an improvement can improve the uncertainty of the telescope. The uncertainty of the Pcal in O3GK was estimated to be 3% [4], which was larger than that of LIGO (0.75 %) [3]. This situation indicates the possibility of improving the uncertainty.

These three points are our Pcal upgrade points for O4.

3. Upgrades for O4

3.1 Installation of remote-controllable mirrors

For issue A, piezo actuators were installed on a mirror mount holding a mirror to enable the Pcal laser beam in A chamber to remotely control the alignment at the point just before the long vacuum pipe. The actuators are vacuum-compatible piezo linear actuators (picomotors) provided by Newport (ultrahigh-vacuum model). They have travel ranges of 12.7 and 25.4 mm. Figure 4 shows the mirrors with the picomotor-installed mount, which are marked with white tape temporarily. Given that the purpose of the picomotors is to fine tune the beam positions on the ETM on the order of a few mm to a few cm and considering that the mirrors are 3-inch mirrors and the distance to the ETM is 34.9 m, the travel ranges are sufficient. This remote alignment system not only increases the efficiency of the initial alignment but also compensates for alignment changes caused by vacuuming.

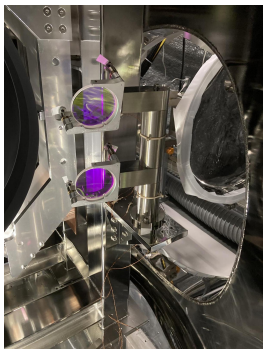

Figure 4: Picomotor-installed mirrors in A chamber. These mirrors align the Pcal beams to the ETM, which is located 34.9 m away, using a vacuum pipe. The remote control system with the picomotors allows for fine alignment adjustment.

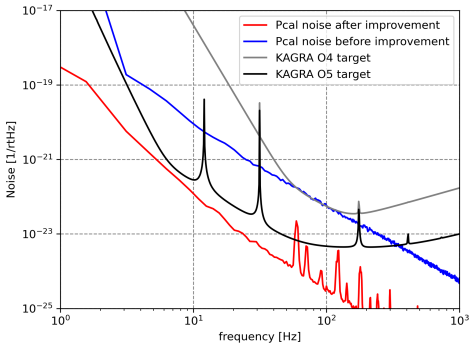

Figure 5: Estimated noise on the main interferometer caused by the Pcal. The noise has been improved by ~50dB, which is sufficiently lower than the target sensitivities of KAGRA.

3.2 Pcal noise hunting and the countermeasures

During the investigation of the Pcal noise, a large unexpected sinusoidal signal was found in the signal to the Pcal OFS system. This signal was finally identified as the noise source. Although the Pcal OFS system is assembled with analog circuits, ports, such as those for reference signals, receive input from the KAGRA digital system through a digital-analog converter (DAC) and anti-imaging (AI) filters (Figure 2). The unexpected signals were ~5 Vpp at ~500 kHz and observed at the input ports of the Pcal OFS analog circuit. This situation indicates that these signals may exert unexpected effects on the OFS system. We found that OP amps (analog devices, AD8622) with an output impedance of 100 Ω in the final stage of the AI circuit caused the unexpected signals owing to their inability to supply sufficient current to the parasitic capacitance of the long cable over 35 m in length between the OFS circuit at the area of A chamber and the AI circuits at the end mirror area. We added a buffer circuit just after the AI circuit to prevent the unexpected signals using AD8672 (analog devices) with 500 Ω output impedance.

The noise in the interferometer caused by the Pcal is shown in Figure 5. Under the laser power-stabilized condition provided by an OFS control loop, the relative intensity noise (RIN) was obtained by measuring the laser power fluctuation with the TxPD1 and TxPD2. Subsequently, using Equation 1 and the following parameters, the mirror displacement noise produced by this Pcal laser was calculated and divided by the baseline length of 3000 m to yield the strain-equivalent noise. The parameters used were $\theta = 0.755\ ^\circ$, $M = 22.945$ kg, and $c = 2.99792458 \times 10^8$ m/s. $(\vec{a} \cdot \vec{b})M/I$ was ignored because its value is sufficiently small relative to 1 when the beam positions are adjusted well. In addition, given that the required DC laser power depends on the sensitivity of the interferometer, a value of 1 W is assumed for each path. This value is similar to that used or planned to be used in O3GK (3.2 W) and O4 (1 W). No reference signal was injected during the noise measurement. The result shows that the sensitivity of the interferometer could have been limited by the Pcal before this improvement; however, with the added buffer circuit, the noise is now sufficiently low. Note that if the interferometer sensitivity is as good as designed, the Pcal reference

signal can be observed with an adequately large signal-to-noise ratio (SNR) in the interferometer even with a low laser power, indicating that the noise caused by the Pcal laser can be reduced.

3.3 Uncertainty improvement with an updated integrating sphere calibration procedure

A close investigation of the integrating sphere calibration data in O3GK showed that the data variability in the long-term monitoring was greater than expected. We focused on the two points listed below to identify the causes of the variation and implement countermeasures. Although the overall results of the data acquired and countermeasures taken for O4 will become clear in the future, the investigations and countermeasures for these two points are described in this section.

a. Temperature dependence of integrating spheres

b. Conditions of beam injection into an integrating sphere

For point a, we monitored the time evolution of the WSK output in our laboratory by injecting a laser into the WSK [7]. A silicon diode thermometer was attached to the sensor part of the WSK and was simultaneously used to monitor the temperature of the WSK. The results are shown in Figure 6, which implies that the temperature change stabilizes ∼1 h after the laser injection and that output of the WSK is correlated with the temperature, which may change by ∼10%. In our integrating sphere calibration, we always compare two integrating spheres. Therefore, if the time variation is similar at the two integrating spheres, the temperature dependence effect is small. Based on these results, we decided to provide a warming-up time of 1 h in our integrating sphere calibration procedure.

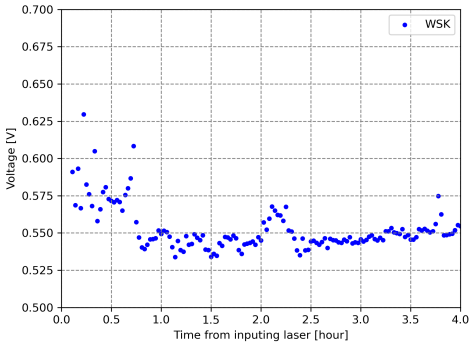

(a) Output voltage of the WSK.

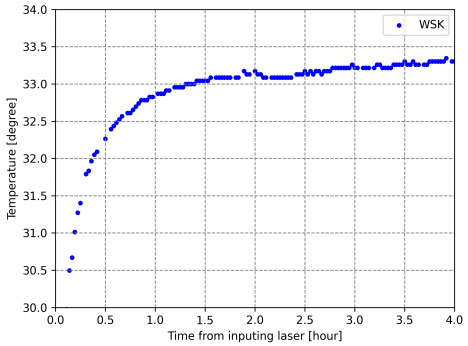

(b) Temperature changes of the WSK.

Figure 6: Time variation of the output voltage and temperature of the WSK after the injection of a power-stabilized laser. The temperature of the WSK increases immediately after the laser injection, and the output voltage of the WSK decreases accordingly. These large time changes stabilize in ∼1 h.

Regarding point b, the output of the laser power sensors of integrating spheres is generally supposed to be independent of the angle and polarization of the incident laser and the position of the incident laser if it is well inside the edge of the incident port. However, our research shows that these factors must also be considered to achieve a subpercent uncertainty in the future. As described in our study [8], the effect of the incident angle becomes significant from approximately −10 °, with an effect of ∼8 % in the worst case scenario. Even at an incident angle between +5 ° and −5 °, the

effect of ~0.1 % is possible. The dependence on incidence position has also been investigated by the LIGO calibration group and suggests an effect of a few tenths of a percent impact [9]. For O4, a mark or positioning mechanism is applied in the Tx/Rx module and the calibration measurement setup for the WSK such that the incident angles are ~ 0 ° and the beam positions are at the center of the port at each calibration measurement to reduce the influence of effects.

4. Conclusion

As the number of observed GW events increases, the calibration of GW telescopes becomes increasingly important. The KAGRA interferometer is calibrated using the Pcal, which is similar to the calibration systems of LIGO and Virgo. We have upgraded the Pcal after the O3GK.

The three main upgrades, namely, an improved laser beam alignment system, reduced laser power noise, and tasks for improving the calibration uncertainty of the Pcal itself, were completed before O4. In particular, the laser noise was reduced by ~50 dB and is sufficiently lower than the target sensitivity of KAGRA. The overall uncertainty of the Pcal, including the effect of the improvements above, will be obtained after the ongoing O4 and analysis and is anticipated to be better than the 3 % uncertainty obtained in the O3GK.

The Pcal is a calibration method used in GW telescopes for many years. It has the potential for reducing the uncertainty. Given that improving the calibration accuracy, precision, and reliability of telescopes is an ongoing and future challenge, we will further improve the Pcal and develop other new calibration methods, such as a gravity field calibrator (Gcal) [10].

References

[1] B.P.Abbott et al., 2016 *PRL*, 119.161101

[2] B.P.Abbott et al., 2017 *Astrophys J*, 848 L12

[3] S.Karki et al., 2016 *Rev Sci Instrum*, 87, 114503

[4] T.Akutsu et al., 2021 *PETP*, 05A102

[5] Bin-Hua Hsieh, 2018 *Master thesis of U.Tokyo*

[6] S.Karki, D. Bhattacharjee, R.L. Savage, 2022 *Galaxies*, 10, 42

[7] K.Ito, 2021 *Master thesis of U.Toyama*

[8] Shingo Fujii on behalf of the KAGRA collaboration, 2023 *ICRC*

[9] M.Spidell et al, 2021 *Metrologia* 58 055011

[10] Rishabh Bajpai on behalf of the KAGRA collaboration, 2023 *ICRC*

PoS(ICRC2023)1549

Full Authors List: KAGRA Collaboration

H. Abe[1], T. Akutsu[2,3], M. Ando[4,5], M. Aoumi[6], A. Araya[7], N. Aritomi[8], Y. Aso[2,9], S. Bae[10], R. Bajpai[2], K. Cannon[5], Z. Cao[11], R.-J. Chang[12], A. H.-Y. Chen[13], D. Chen[14], H. Chen[15], Y. Chen[15], A. Chiba[16], R. Chiba[17], C. Chou[18], M. Eisenmann[2], S. Fujii[17], I. Fukunaga[19], D. Haba[1], S. Haino[20], W.-B. Han[21], H. Hayakawa[6], K. Hayama[22], Y. Himemoto[23], N. Hirata[2], C. Hirose[24], S. Hoshino[24], H.-F. Hsieh[25], C. Hsiung[26], S.-C. Hsu[27,25], D. C. Y. Hui[28], K. Inayoshi[29], Y. Itoh[19,30], M. Iwaya[17], H.-B. Jin[31,32], K. Jung[33], T. Kajita[34], M. Kamiizumi[6], N. Kanda[30,19], J. Kato[16], T. Kato[17], S. Kim[28], N. Kimura[6], T. Kiyota[19], K. Kohri[35], K. Kokeyama[36], K. Komori[5,4], A. K. H. Kong[25], N. Koyama[24], J. Kume[5], S. Kuroyanagi[38,37], S. Kuwahara[5], K. Kwak[33], S. Lai[18], H. W. Lee[39], R. Lee[15], S. Lee[40], M. Leonardi[41,2], K. L. Li[12], L. C.-C. Lin[12], C-Y. Lin[42], E. T. Lin[25], G. C. Liu[26], L.-T. Ma[25], K. Maeda[16], M. Matsuyama[19], M. Meyer-Conde[19], Y. Michimura[43,5], N. Mio[44], O. Miyakawa[6], S. Miyamoto[17], S. Miyoki[6], S. Morisaki[17], Y. Moriwaki[16], M. Murakoshi[45], K. Nakamura[2], H. Nakano[46], T. Narikawa[17], L. Nguyen Quynh[47], Y. Nishino[2,48], A. Nishizawa[5], K. Obayashi[45], J. J. Oh[49], K. Oh[28], M. Ohashi[6], M. Ohkawa[24], K. Oohara[50,51], Y. Oshima[4], S. Oshino[6], M. A. Page[2], K.-C. Pan[15,25], J. Park[40], F. E. Peña Arellano[6], S. Saha[25], K. Sakai[52], T. Sako[16], R. Sato[24], S. Sato[16], Y. Sato[16], T. Sawada[6], Y. Sekiguchi[53], L. Shao[29], Y. Shikano[54,55], K. Shimode[6], H. Shinkai[56], J. Shiota[45], K. Somiya[1], T. Suzuki[24], T. Suzuki[1], H. Tagoshi[17], H. Takahashi[57], R. Takahashi[2], A. Takamori[7], K. Takatani[19], H. Takeda[58], M. Takeda[19], M. Tamaki[17], K. Tanaka[59], S. J. Tanaka[45], T. Tanaka[58], A. Taruya[60], T. Tomaru[2], K. Tomita[19], T. Tomura[6], A. Toriyama[45], A. A. Trani[5], S. Tsuchida[61], N. Uchikata[17], T. Uchiyama[6], T. Uehara[62], K. Ueno[5], T. Ushiba[6], M. H. P. M. van Putten[63], H. Wang[4], T. Washimi[2], C. Wu[15], H. Wu[15], K. Yamamoto[16], M. Yamamoto[16], T. Yamamoto[6], T. S. Yamamoto[37], S. Yamamura[17], R. Yamazaki[45], L.-C. Yang[18], Y. Yang[18], S.-W. Yeh[15], J. Yokoyama[5,4], T. Yokozawa[6], H. Yuzurihara[6], Y. Zhao[17,2], Z.-H. Zhu[11,64]

[1]Graduate School of Science, Tokyo Institute of Technology, 2-12-1 Ookayama, Meguro-ku, Tokyo 152-8551, Japan. [2]Gravitational Wave Science Project, National Astronomical Observatory of Japan, 2-21-1 Osawa, Mitaka City, Tokyo 181-8588, Japan. [3]Advanced Technology Center, National Astronomical Observatory of Japan, 2-21-1 Osawa, Mitaka City, Tokyo 181-8588, Japan. [4]Department of Physics, The University of Tokyo, 7-3-1 Hongo, Bunkyo-ku, Tokyo 113-0033, Japan. [5]Research Center for the Early Universe (RESCEU), The University of Tokyo, 7-3-1 Hongo, Bunkyo-ku, Tokyo 113-0033, Japan. [6]Institute for Cosmic Ray Research, KAGRA Observatory, The University of Tokyo, 238 Higashi-Mozumi, Kamioka-cho, Hida City, Gifu 506-1205, Japan. [7]Earthquake Research Institute, The University of Tokyo, 1-1-1 Yayoi, Bunkyo-ku, Tokyo 113-0032, Japan. [8]LIGO Hanford Observatory, Richland, WA 99352, USA. [9]The Graduate University for Advanced Studies (SOKENDAI), 2-21-1 Osawa, Mitaka City, Tokyo 181-8588, Japan. [10]Korea Institute of Science and Technology Information (KISTI), 245 Daehak-ro, Yuseong-gu, Daejeon 34141, Republic of Korea. [11]Department of Astronomy, Beijing Normal University, Xinjiekouwai Street 19, Haidian District, Beijing 100875, China. [12]Department of Physics, National Cheng Kung University, No.1, University Road, Tainan City 701, Taiwan. [13]Institute of Physics, National Yang Ming Chiao Tung University, 101 Univ. Street, Hsinchu, Taiwan. [14]Kamioka Branch, National Astronomical Observatory of Japan, 238 Higashi-Mozumi, Kamioka-cho, Hida City, Gifu 506-1205, Japan. [15]Department of Physics, National Tsing Hua University, No. 101 Section 2, Kuang-Fu Road, Hsinchu 30013, Taiwan. [16]Faculty of Science, University of Toyama, 3190 Gofuku, Toyama City, Toyama 930-8555, Japan. [17]Institute for Cosmic Ray Research, KAGRA Observatory, The University of Tokyo, 5-1-5 Kashiwa-no-Ha, Kashiwa City, Chiba 277-8582, Japan. [18]Department of Electrophysics, National Yang Ming Chiao Tung University, 101 Univ. Street, Hsinchu, Taiwan. [19]Department of Physics, Graduate School of Science, Osaka Metropolitan University, 3-3-138 Sugimoto-cho, Sumiyoshi-ku, Osaka City, Osaka 558-8585, Japan. [20]Institute of Physics, Academia Sinica, 128 Sec. 2, Academia Rd., Nankang, Taipei 11529, Taiwan. [21]Shanghai Astronomical Observatory, Chinese Academy of Sciences, 80 Nandan Road, Shanghai 200030, China. [22]Department of Applied Physics, Fukuoka University, 8-19-1 Nanakuma, Jonan, Fukuoka City, Fukuoka 814-0180, Japan. [23]College of Industrial Technology, Nihon University, 1-2-1 Izumi, Narashino City, Chiba 275-8575, Japan. [24]Faculty of Engineering, Niigata University, 8050 Ikarashi-2-no-cho, Nishi-ku, Niigata City, Niigata 950-2181, Japan. [25]Institute of Astronomy, National Tsing Hua University, No. 101 Section 2, Kuang-Fu Road, Hsinchu 30013, Taiwan. [26]Department of Physics, Tamkang University, No. 151, Yingzhuan Rd., Danshui Dist., New Taipei City 25137, Taiwan. [27]Department of Physics, University of Washington, 3910 15th Ave NE, Seattle, WA 98195, USA. [28]Department of Astronomy and Space Science, Chungnam National University, 9 Daehak-ro, Yuseong-gu, Daejeon 34134, Republic of Korea. [29]Kavli Institute for Astronomy and Astrophysics, Peking University, Yiheyuan Road 5, Haidian District, Beijing 100871, China. [30]Nambu Yoichiro Institute of Theoretical and Experimental Physics (NITEP), Osaka Metropolitan University, 3-3-138 Sugimoto-cho, Sumiyoshi-ku, Osaka City, Osaka 558-8585, Japan. [31]National Astronomical Observatories, Chinese Academic of Sciences, 20A Datun Road, Chaoyang District, Beijing, China. [32]School of Astronomy and Space Science, University of Chinese Academy of Sciences, 20A Datun Road, Chaoyang District, Beijing, China. [33]Department of Physics, Ulsan National Institute of Science and Technology (UNIST), 50 UNIST-gil, Ulju-gun, Ulsan 44919, Republic of Korea. [34]Institute for Cosmic Ray Research, The University of Tokyo, 5-1-5 Kashiwa-no-Ha, Kashiwa City, Chiba 277-8582, Japan. [35]Institute of Particle and Nuclear Studies (IPNS), High Energy Accelerator Research Organization (KEK), 1-1 Oho, Tsukuba City, Ibaraki 305-0801, Japan. [36]School of Physics and Astronomy, Cardiff University, The Parade, Cardiff, CF24 3AA, UK. [37]Department of Physics, Nagoya University, ES building, Furocho, Chikusa-ku, Nagoya, Aichi 464-8602, Japan. [38]Instituto de Fisica Teorica UAM-CSIC, Universidad Autonoma de Madrid, 28049 Madrid, Spain. [39]Department of Computer Simulation, Inje University, 197 Inje-ro, Gimhae, Gyeongsangnam-do 50834, Republic of Korea. [40]Technology Center for Astronomy and Space Science, Korea Astronomy and Space Science Institute (KASI), 776 Daedeokdae-ro, Yuseong-gu, Daejeon 34055, Republic of Korea. [41]Department of Physics, University of Trento, via Sommarive 14, Povo, 38123 TN, Italy. [42]National Center for High-performance computing, National Applied Research Laboratories, No. 7, R&D 6th Rd., Hsinchu Science Park, Hsinchu City 30076, Taiwan. [43]LIGO Laboratory , California Institute of Technology, 1200 East California Boulevard, Pasadena, CA 91125, USA. [44]Institute for Photon Science and Technology, The University of Tokyo,

2-11-16 Yayoi, Bunkyo-ku, Tokyo 113-8656, Japan. [45]Department of Physical Sciences, Aoyama Gakuin University, 5-10-1 Fuchinobe, Sagamihara City, Kanagawa 252-5258, Japan. [46]Faculty of Law, Ryukoku University, 67 Fukakusa Tsukamoto-cho, Fushimi-ku, Kyoto City, Kyoto 612-8577, Japan. [47]Department of Physics and Astronomy, University of Notre Dame, 225 Nieuwland Science Hall, Notre Dame, IN 46556, USA. [48]Department of Astronomy, The University of Tokyo, 7-3-1 Hongo, Bunkyo-ku, Tokyo 113-0033, Japan. [49]National Institute for Mathematical Sciences, 70 Yuseong-daero, 1689 Beon-gil, Yuseong-gu, Daejeon 34047, Republic of Korea. [50]Graduate School of Science and Technology, Niigata University, 8050 Ikarashi-2-no-cho, Nishi-ku, Niigata City, Niigata 950-2181, Japan. [51]Niigata Study Center, The Open University of Japan, 754 Ichibancho, Asahimachi-dori, Chuo-ku, Niigata City, Niigata 951-8122, Japan. [52]Department of Electronic Control Engineering, National Institute of Technology, Nagaoka College, 888 Nishikatakai, Nagaoka City, Niigata 940-8532, Japan. [53]Faculty of Science, Toho University, 2-2-1 Miyama, Funabashi City, Chiba 274-8510, Japan. [54]Graduate School of Science and Technology, Gunma University, 4-2 Aramaki, Maebashi, Gunma 371-8510, Japan. [55]Institute for Quantum Studies, Chapman University, 1 University Dr., Orange, CA 92866, USA. [56]Faculty of Information Science and Technology, Osaka Institute of Technology, 1-79-1 Kitayama, Hirakata City, Osaka 573-0196, Japan. [57]Research Center for Space Science, Advanced Research Laboratories, Tokyo City University, 8-15-1 Todoroki, Setagaya, Tokyo 158-0082, Japan. [58]Department of Physics, Kyoto University, Kita-Shirakawa Oiwake-cho, Sakyou-ku, Kyoto City, Kyoto 606-8502, Japan. [59]Institute for Cosmic Ray Research, Research Center for Cosmic Neutrinos, The University of Tokyo, 5-1-5 Kashiwa-no-Ha, Kashiwa City, Chiba 277-8582, Japan. [60]Yukawa Institute for Theoretical Physics (YITP), Kyoto University, Kita-Shirakawa Oiwake-cho, Sakyou-ku, Kyoto City, Kyoto 606-8502, Japan. [61]National Institute of Technology, Fukui College, Geshi-cho, Sabae-shi, Fukui 916-8507, Japan. [62]Department of Communications Engineering, National Defense Academy of Japan, 1-10-20 Hashirimizu, Yokosuka City, Kanagawa 239-8686, Japan. [63]Department of Physics and Astronomy, Sejong University, 209 Neungdong-ro, Gwangjin-gu, Seoul 143-747, Republic of Korea. [64]School of Physics and Technology, Wuhan University, Bayi Road 299, Wuchang District, Wuhan, Hubei, 430072, China.

PoS(ICRC2023)1549